Revista Colombiana de Física, Vol. 43, No. 2 de 2011.

Tomography With Medipix2 Semiconductor Pixel Detector

Tomografía Con El Detector De Pixel Semiconductor Medipix2

C. F. Roa [a], B. Gómez. [a]

[a] *Universidad de los Andes, A.A.4976, Bogotá, Colombia.*

Recibido 10.04.10; Aceptado 13.01.11; Publicado en línea 04.09.11.

Resumen

El detector de pixel Medipix2, desarrollado en CERN, presenta características que lo hacen interesante para aplicaciones médicas que demandan producción de imágenes de alta resolución. Entre sus características están 256 x 256 pixeles, cada uno de tamaño de 50 µm x 50 µm con su propia electrónica por pixel con analizador de monocanal. Se realizaron mediciones en la Universidad de los Andes, Bogotá, Laboratorio de Física de Altas Energías, para caracterizar y calibrar el detector Medipix2. Para la calibración de energía se utilizaron las líneas características de rayos-X de tubos con ánodo de Cu y de Mo. A los datos crudos se aplicaron correcciones de campo plano y de endurecimiento del haz. La calibración de energía del detector y su capacidad de aplicar una ventana de energía se utilizaron para tomar radiografías a diferentes energías. Se obtuvo un conjunto de proyecciones para dos fantasmas y para un objeto real, para cada uno 200 proyecciones al rotarlo con un motor de paso de precisión para realizar su reconstrucción tomográfica por tajadas, que apiladas dieron imágenes tridimensionales del interior de los objetos y fueron comparadas con la estructura real de los mismos.

Palabras clave: Medipix; Imágenes con Rayos-X; Tomografía.

Abstract

The Medipix2 pixel detector, developed at CERN, presents features that make it interesting for medical applications that demand high resolution imaging, among them 256 x 256 pixels, each one 50 µm x 50 µm in size and its own pixel electronics with single channel analyzer. Measurements were done at the Universidad de los Andes, Bogotá, High Energy Physics Laboratory, to characterize and calibrate the Medipix2 detector. For the energy calibration the characteristic lines of Cu and Mo X-ray tubes were used. Flat field and beam hardening corrections were applied to the raw data. The energy calibration of the detector and its capability of setting an energy window were used to take radiographies at different energies. A set of projections was obtained for two phantoms and a real object, for each one 200 projections, by rotating them with a precision step motor, to perform their tomographical reconstruction, stepwise in slices that together gave 3-dimensional images of the interior of the objects and were compared with the real structure of the objects.

Keywords: Medipix, X-ray Imaging, Tomography

PACS: 87.57.Q-.

1. Introduction

Medipix2 is a high definition, energy sensitive, photon counting pixel detector, designed for biomedical imaging. We report here on the use of the Medipix2 detector for tomography as experienced at the Universidad de los Andes, Bogotá. [1]

* bgomez@uniandes.edu.co

Tomographies are generated from sequences of digital radiographies acquired for different angles of incidence of X-rays. For small objects in front of the Medipix sensor, a precision step motor rotates the object in equal azimuthal steps giving a sequence of 200 radiographies in 360°. The tomographical reconstruction requires high quality projections obtained after processing the Medipix raw data. A description of the Medipix detector and the procedures applied to obtain high quality images are presented in what follows.

6. The Medipix2 Detector [2], [3]

The Medipix2 is a 16120 µm × 14111 µm chip, composed by a 300 µm thick Si sensors arranged as an array of 256 × 256 pixels, each one of 55 µm × 55 µm, with a total sensitive area of 1.98 cm^2. The non sensitive area of the chip measures 2040 µm × 14111 µm and has the wire-bonding pads, biasing Digital to Analog Converters (DACs) and control logic. See fig. 1.

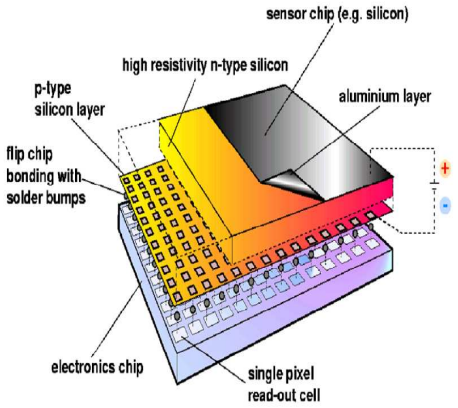

Fig. 1: Schematic of the Medipix2 pixel detector with the sensor chip and the electronics chip connected via bump bonds. [3]

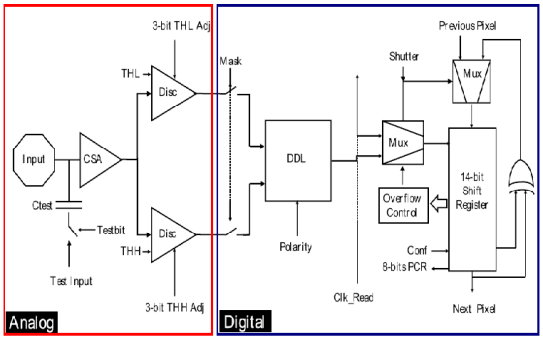

Fig. 2: Schematic of one Medipix2 pixel showing the analog (red) and digital (blue) parts. [3]

The electronics for each pixel has an analog and a digital part, as can be seen in fig. 2.

The analog part of the pixel has a test capacitance, the Charge Sensitive Amplifier (CSA) and the two discriminators. The input is the current pulse that comes from the semiconductor detector upon the interaction of a photon or a charged particle with the crystal.

The test capacitance is used to input a known amount of charge to the pixel to test the settings. The CSA integrates the input charge and shapes it. It also has a compensation for positive or negative leakage currents.

The two discriminators are equal, but the threshold voltage on each of them can be set individually. The high and low thresholds are set by an 8-bit DAC for all the pixels of the matrix.

The digital part of the pixel has the Double Discriminator Logic (DDL), the Shift Register Counter (SR/C) and the Pixel Configuration Register (PCR). The DDL allows setting the detector in single threshold mode or in window mode.

The detector can be set in a single threshold mode, by setting the high threshold (THH) lower than the low threshold (THL). In this setting, the pulses with a voltage higher than THL are counted. On the window mode, an energy window is set with the THL and THH voltages. The pulses with a voltage higher than THL and lower than THH are counted. The rest of the pulses are discarded.

To connect the Medipix2 detector to a personal computer we use the "USB Interface", developed at the Institute of Experimental and Applied Physics (IEAP) of the Czech Technical University in Prague [4]. This interface allows to readout the pixel matrix and to control the acquisition and its parameters. It has an internal source of variable bias voltage with leakage current monitor that allows setting voltages from 5 to 100 V. This is the voltage along the semiconductor sensor that separates the electron hole pair for the detection of one of them.

Data acquisition with Medipix2 via the USB Interface is controlled by the Pixelman software, developed at the IEAP. [4] In addition to the basic control of the Medipix2 chip, Pixelman offers a series of useful plugins, which allow performing operations additional to the acquisition, such as coincidence control, beam hardening correction and more complex measurements.

7. Preliminary Measurements [5] , [6]

Prior to the acquisition of radiographies for tomography a series of measurements were done with the Medipix2 detector for optimum quality of the images, among them

threshold equalization, energy calibration, flat field correction and beam hardening correction.

3.1 Threshold Equalization [2]

To have a more unified threshold throughout the 256 x 256 matrix threshold equalization is required. This is the procedure by which the 3-bit DAC value is set for the low threshold (THL) and high threshold (THH) branch for each pixel.

The purpose is to minimize the threshold variation due to differences in the transistors and power consumption. The 3-bit DAC controls the amount of current that is added to the output of the discriminator and is unique for each threshold and each pixel. At the end of each discriminator, there is a mask bit that allows discarding the information from noisy or defective pixels.

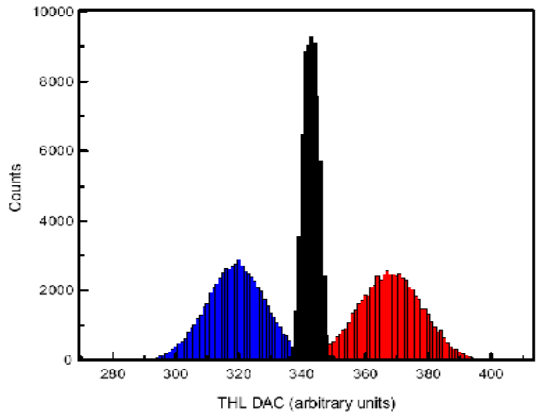

Fig. 3: Low threshold equalization distributions before (blue and red distributions) and after equalization (black distribution).

The low threshold equalization uses the noise floor to determine the value of THL DAC at which a pixel stops counting. This is done once with the 3-bit current DAC set to 000 (red distribution in fig. 3). Then the DAC is set to 111 (blue distribution in fig. 3).

As the behavior of the threshold is linear, an interpolation can be done to determine for each pixel the 3-bit current DAC that minimizes the dispersion (black distribution in fig. 3).

3.2 Energy Calibration [5], [6], [7]

For energy calibration the Medipix2 was illuminated with a known X-ray or gamma ray spectrum and a THL DAC scan was performed, rising the low threshold. The points at which the rate of change of the counts has peaks are the points at which the characteristic lines of the source lie.

The known X-ray source was the PHYWE X-ray unit with two different tubes, Mo and Cu anodes, giving the characteristic Kα and Kβ spectrum lines of these elements as incident X-rays of known energy for calibration. The spectrum for each tube was measured applying Bragg's law.

3.3 Flat Field Correction [8]

The flat field correction is used to eliminate the distortion of the image due to the difference in efficiency among pixels. This correction can also compensate the negative effects of a non-uniform radiation field. After correcting with flat field, a radiography displays details of the sample with higher contrast and the statistical variation throughout the image is reduced.

3.4 Beam Hardening Correction [4], [8]

The attenuation of X-rays depends on the beam energy. In the Medipix2 pixel detector used for transmission radiography the spectrum in each pixel is unique and depends on the composition of the sample it passed through.

The energy dependence of the absorption causes the spectrum to be harder in the thicker parts. As each pixel has a unique efficiency, a correction is applied for the beam hardening effect.

For flat absorbers of various thicknesses a "Signal to Thickness Calibration" (STC) is performed. The absorbers can be aluminum or plastic foils. This calibration is applied to the radiographical images, converting counts into thicknesses of the object being studied.

8. Tomographical Imaging with Medipix2

4.1 Experimental Setup

The Medipix2 was placed inside the PHYWE X-ray unit using the Medipix2 support designed and constructed at the Universidad de los Andes. For the radiographies the Mo tube with a voltage of 35 kV and current of 1 mA was used. The detector was placed in front of the 5 mm collimator at a distance of 390 mm.

The sample was placed at 355 mm from the collimator. An exposure time of 2.5 seconds was used for the radiographies. A precision step motor, controlled via a LabView program, rotated the sample after each projection was taken (see fig. 4). It took from five to ten minutes to acquire 200 projections in 360°.

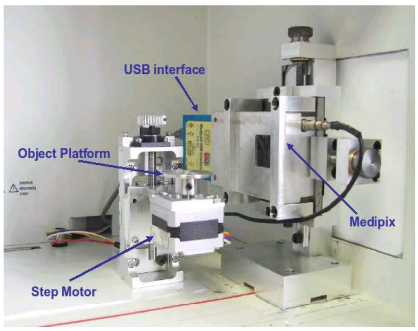

Fig.4: Experimental setup for tomography imaging, inside the PHYWE X-ray unit: The precision step motor rotates the object platform in front of the Medipix2 detector.

4.2 Tomographical Reconstruction [9], [10], [11]

Three dimensional images of the interior of the object being studied are generated, from a series of two dimensional transmission radiographies.

We follow the mathematical formulation of the procedure for tomographical reconstruction by Allan McLeod Cormack. It is based on the Fourier Slice Theorem and is implemented with the use of the Fast Fourier Transform.

The attenuation of X-rays as they pass through the object gives the radiographical projections P(θ,t) along the t line for angle θ in the range from 0 to π, as is shown in fig. 5. For a slice of the object, the function f(x,y) gives the attenuation coefficient at each point (x,y) of its volume, and it is obtained by the inverse Fourier transform of the series of projections P(θ,t).

After reconstruction of the interior of the slices, the set of piled slices gives a three dimensional image of the interior of the object, a tomography.

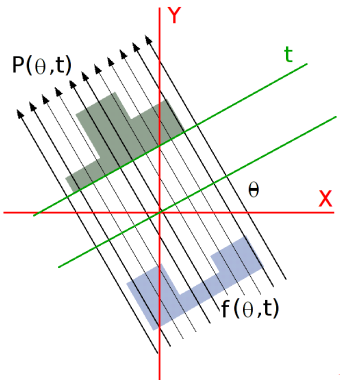

Fig.5: Geometry definition for tomographical reconstruction. The function f(x, y) represents the object and P(θ, t) its projection.

The reconstruction of the sample from the projections was done with Octopus 8.3, a commercial tomography reconstruction package for CT, developed at the Centre for X-ray Tomography of the Ghent University. [12]

4.3 Cone Shell Tomography [1]

200 radiographical projections of the shell were acquired rotating it 360°. This was done separately for the lower part and for the upper part of the cone shell.

Flat field and beam hardening corrections were applied to the projections and the tomographical reconstruction process gave the three dimensional internal structure of the cone shell. Fig. 6 presents a photograph of the cone shell of 30 mm length and two projections of the tomographical reconstruction showing part of the internal structure of the cone shell.

Since the Medipix2 pixel detector gives an array of 256 x 256 pixels, from a single transmission radiography we obtain 256 slice projections of the object. The sequence of 200 radiographies for different angles of incidence of the X-rays gives 200 projections of 256 slices, and out of these we reconstruct the three dimensional tomographic image. Fig. 7 shows a selection of four reconstructed slices, four cross sections of the cone shell. Fig. 8 shows the three dimensional tomographies of the lower and upper parts of the cone shell.

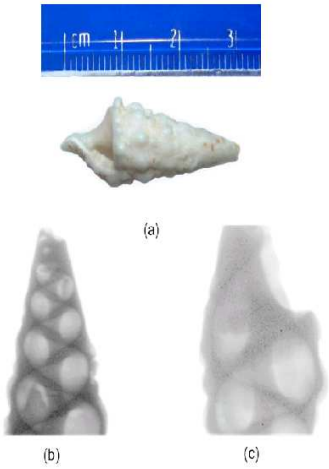

Fig. 6: Photograph (a), STC-corrected projection of lower part (b) and STC-corrected projection of upper part (c) of the cone shell.

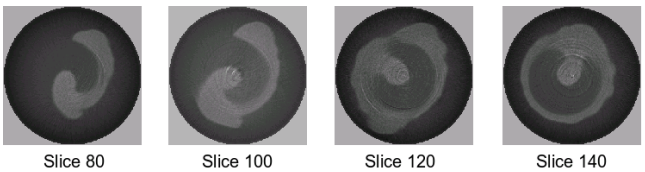

Fig. 7: Selection of four cross sections of the cone shell obtained as tomographical reconstructions of two-dimensional projections.

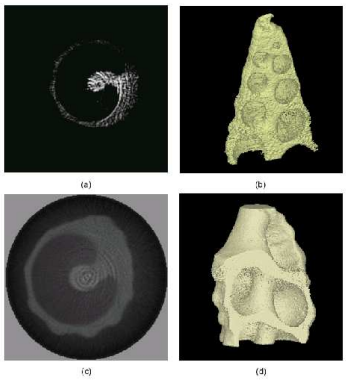

Fig. 8: Reconstructed slice of lower part (a), multi-surface render of lower part (b), reconstructed slice of upper part (c) and multi-surface render of upper part (d) of the cone shell.

9. Final Discussion

After performing an energy calibration of the detector, the energy window feature of the Medipix2 was used to take radiographies at different energies. For tomography for each object a series of 200 radiographical projections in 360 were acquired. The flat field and beam hardening correction were implemented to the projections. The Octopus 8.3 software was used for the reconstruction process.

The size of the focus of the X-ray tube (1 mm) and the low intensity of the beam were not a limitation for the quality of the reconstructed images. However, if higher resolution is needed, it is essential to increment the distance between the source and the detector, or to use an X-ray tube with a smaller focus.

Medipix2 is capable of giving images with micrometer resolution. For such resolution a micro focus X-ray tube is required.

10. Acknowledgements

For its support to this work, we thank Universidad de los Andes, Bogotá, Colombia; Medipix3 Collaboration at CERN; Institute of Experimental and Applied Physics (IEAP), Czech Technical University in Prague; High Energy Latin-American European Network (HELEN); COLCIENCIAS, Colombia.

References

[1] C. F. Roa. Tomography with Medipix2 Semiconductor Pixel Detector. Thesis. Physics Department. Universidad de los Andes. Bogota. November 2008.

[2] X. Llopart, M. Campbell, D. San Segundo, E. Pernigotti, and R. Dinapoli. Medipix2, a 64k Pixel Read Out Chip with 55 μm Square Elements Working in Single Photon Counting Mode. IEEE, 3(1), November 2001.

[3] X. Llopart. Design and Characterization of 64K Pixels Chips Working in Single Photon Processing Mode. PhD thesis, CERN, 2006.

[4] Department of Applied Physics and Technology IEAP. Medipix in IEAP. http://aladdin.utef.cvut.cz/ofat/index.html

[5] C. Lebel. Energy Calibration of the Low Threshold of Medipix USB. Université de Montréal, 2007.

[6] M. Fierdele, D. Greiffenberg, Et Al. Energy Calibration Measurements of Medipix2. Nuclear Instruments and Methods in Physics Research A 536, pages 75-79, March 2008.

[7] L. Tlustos, R. Ballabriga, M. Campbell, Et Al. Imaging Properties of the Medipix2 System Exploiting Single and Dual Energy Thresholds. IEEE, pages 2155–2159, July 2004.

[8] J. Jakubek. "Data Processing and Image Reconstruction Methods for Pixel Detectors". Nuclear Instruments and Methods in Physics Research A, Volume 576, Issue 1, 11 June 2007, Pages 223-234.

[9] A. M. Cormack. Representation of a Function by Its Line Integrals, with Some Radiological Applications. Journal of Applied Physics, 34(2722), September 1963.

[10] A. M. Cormack. Representation of a Function by Its Line Integrals, with Some Radiological Applications II. Journal of Applied Physics, 35(2908), October 1964.

[11] A. C. Kak and M. Slaney. Principles of Computerized Tomographic Imaging. IEEE Press, 1988.

[12] XrayLAB. Octopus 8.3 Manual. Ghent University. 2008.